The Journal of Physical Chemistry A

 VOLUME 103, NUMBER 30, JULY 29, 1999

# LETTERS

## Clustering of Acetic Acid by Association of Hydrogen-Bonded Dimers: Spectroscopic Observation of Multicomponent (Ne)·($C_6H_6$)·($CH_3COOH$)$_n$ Clusters

**I. N. Germanenko and M. S. El-Shall***

*Department of Chemistry, Virginia Commonwealth University, Richmond, Virginia 23284-2006*

*Received: April 30, 1999; In Final Form: June 4, 1999*

Resonant two-photon ionization (R2PI) spectra of benzene−acetic acid binary clusters $BA_n$, with $n = 1-6$ are reported. The results indicate that cluster formation from acetic acid vapor proceeds mainly via the association of preformed hydrogen-bonded dimers. The spectral shift of the BA complex is consistent with $\pi$-hydrogen bonding interaction with the benzene ring. The spectral shifts of the $BA_2$ and $BA_3$ clusters are consistent with a predominantly dispersion interaction which is enhanced upon electronic excitation of the benzene molecule. Spectroscopic evidence for the formation of (Ne)·($C_6H_6$)·($CH_3COOH$)$_n$ clusters, with $n =$ 4 and 6, is presented. The direction and magnitude of the spectral shift indicate that the $C_6H_6\cdots$Ne and the $C_6H_6\cdots(CH_3COOH)_n$ structures are retained in the multicomponent clusters, suggesting no perturbations due to the weak $C_6H_6\cdots$Ne interaction.

### 1. Introduction

Gas-phase binary clusters composed of nonpolar aromatics and polar or hydrogen-bonded molecules constitute valuable models to study the role of intermolecular interactions in the evolution of the rich equilibrium and dynamical behaviors known for the condensed phase systems.[1−6] Some examples of these systems include clusters of a benzene molecule with water,[7−10] methanol,[11] and acetonitrile[12] molecules. The study of these clusters provides microscopic information which can lead to a molecular level understanding of many important condensed phase phenomena such as bulk solvation, solvent caging, diffusion, nucleation, microphase separation, and phase transitions.

Benzene−acetic acid binary clusters ($B_mA_n$) represent an interesting subclass of the aromatic−polar clusters where the polar molecules are known to form stable dimers in the gas phase. Dimerization of acetic acid has been extensively studied in the gas phase for more than fifty years.[13−32] Due to the stability of the cyclic dimer involving two hydrogen bonds ($\Delta H° \approx -14$ kcal/mol), it is generally assumed that the dimer is the only important associated species in the vapor phase of acetic acid.[16] Thus, the vapor is considered as an equilibrium mixture of monomers and cyclic dimers with no contributions from higher-order clusters.[21] However, several reports have provided evidence for the existence of acetic acid polymers larger than dimers in the vapor phase.[14,15,19,22] Questions regarding the structures of higher-order clusters and whether the liquid contains chainlike, hydrogen-bonded oligomers or cyclic dimers remain unsolved.[24,26,27,31,32]

Fundamental insight into the intermolecular interactions among acetic acid molecules and between acetic acid clusters and benzene can be obtained by studying the binary $BA_n$ clusters containing a single benzene molecule and multiple acetic acid molecules. Here we report a spectroscopic study of the binary $BA_n$ clusters with $n = 1$ through 6, using resonant two-photon ionization, time-of-flight mass spectrometry (R2PI-TOFMS). The general objective of the present work is to attempt to answer some of the important questions related to the gas-phase association of acetic acid molecules. Among these questions is whether the cluster formation from an associated vapor such as

* Corresponding author.

10.1021/jp991435f CCC: $18.00 
Published on Web 07/14/1999

acetic acid proceeds via clustering of dimers, or monomers formed from dissociated dimers? Another question is how does the strong hydrogen bonding interaction in the acetic acid dimer affect its interaction with the benzene molecule?

In this letter we report the R2PI spectra of the $BA_n$ clusters in the vicinity of the $6_0^1$ transition of the isolated benzene molecule, where benzene serves as a chromophore for the acetic acid clusters. The perturbations imposed on the benzene's $6_0^1$ vibronic transition can provide information on the extent of interactions between benzene and acetic acid molecules in both the ground and excited electronic states. We also present the observation of a benzene·(Ne) complex, and report spectroscopic evidence for the formation of benzene·(Ne)·(acetic acid)$_n$ clusters with $n = 4$ and 6. The $B{\cdot}Ne{\cdot}A_n$ clusters represent novel composite interactions involving the "weak" benzene···Ne and the "stronger" benzene···acetic acid tetramer or hexamer interactions.

## 2. Experimental Section

Binary benzene−acetic acid clusters are generated by pulsed adiabatic expansion in a supersonic cluster beam apparatus.[33,34] The essential elements of the apparatus are jet and beam chambers coupled to a time-of-flight mass spectrometer. The binary clusters are formed in a He−seeded jet expansion, and probed as a skimmed cluster beam in a collision-free high vacuum chamber with a delay between synthesis and probe (i.e., the neutral beam flight time) on the order of 1 ms. During operation, a vapor mixture of benzene and acetic acid (Aldrich, 99.9% purity), in He (ultrahigh purity, Spectra Gases 99.999%) at a pressure of 2−8 atm is expanded through a conical nozzle (100 $\mu$m diameter) in pulses of 200−300 $\mu$s duration at repetition rates of 5−8 Hz. The jet is skimmed and passed into a high vacuum chamber, which is maintained at $8 \times 10^{-8}$ to $2 \times 10^{-7}$ Torr. The collimated cluster beam passes into the ionization region of the TOF mass spectrometer where it intersects a laser pulse from a frequency-doubled dye laser. The tunable radiation is provided by a dye laser (Lambda Physik FL3002) pumped by an excimer laser (Lambda Physik LPX-101). Coumarin 503 (Exciton) dye laser output passes through a $\beta$-$BaB_2O_4$ crystal (CSK Co.) to generate a continuously tunable frequency-doubled output of $10^{-8}$ s pulses. The spatially filtered (using a set of four quartz Pellin-Broca prisms) ultraviolet radiation is adjusted to minimize three photon processes while still providing sufficient ion current (photon power density $\approx 10^6$ W/cm$^2$). The cluster ions formed by the R2PI are electrostatically accelerated in a two-stage acceleration region (300−400 V/cm), and then travel a field-free region (170 cm in length) to a two-stage microchannel-plate detector. Deflection plates are used to compensate for the cluster beam velocity. The TOF spectrum is recorded by digitizing the amplified current output of the detector with a 500 MHz digitizer (LeCroy 9350A) and averaged over 50 pulses.

## 3. Results

Figure 1a presents the one-color, mass-selected R2PI spectra obtained by monitoring the ion intensities in the $BA_n^+$ mass channels with $n = 1$ to 6 as the dye laser is scanned from 38500 to 38 760 cm$^{-1}$. The zero of the scale is taken to be the frequency of the $S_1 \leftarrow S_0$ $6_0^1$ vibronic transition for the bare $C_6H_6$ molecule (38 611 cm$^{-1}$).[35] No characteristic spectral features are observed in the $BA^+$ channel within the frequency shift ($\Delta\nu$) of −100 to +150 cm$^{-1}$. The small doublet observed at $\Delta\nu = -15/-13$ cm$^{-1}$ appears at the same frequencies as the doublet assigned to the origin of the $BA_6$ cluster which, upon photoionization, fragments by the loss of multiple acetic acid molecules and appears in the lower mass channels $BA_n^+$ with $n = 5$, 4, 2, and 1. Far to the blue of the $6_0^1$ transition of benzene, a weak peak located at +152 cm$^{-1}$ can be tentatively assigned to the BA complex as shown in Figure 1b. This origin belongs to a Franck−Condon intermolecular progression [van der Waals (vdw)] with other transitions at 168 and 184 cm$^{-1}$. In addition, other intermolecular vibrations appear at 174, 192, and 209 cm$^{-1}$. The assigned origin (+152 cm$^{-1}$) and all the intermolecular bands appear in the benzene mass channel with stronger intensities than in the $BA^+$ channel as shown in Figure 1b. This indicates efficient loss of acetic acid from the BA complex upon photoionization. From the total ion intensities of identical features in the $BA^+$ and $B^+$ mass channels, the fragmentation efficiency of the $BA^+ \rightarrow B^+$ process can be estimated as 75%.

In the $BA_2^+$ channel, a weak doublet red shifted by 63/61 cm$^{-1}$ is assigned to the origin. This origin possesses a long progression of bands assigned to the excitation of the intermolecular vibrational modes of the $BA_2$ cluster [the first doublet in the progression appears at −56/−54 cm$^{-1}$, followed by three relatively strong (s) bands at −30, −3, and 22 cm$^{-1}$ and two weak (w) bands at 47 and 72 cm$^{-1}$]. Two other long, intermingled vdw progressions are also observed [−44/−42 (s), −26 (w), −9 (w), −12 (s), 12 (s), 28 (s), 55 (w), and 75 (w) cm$^{-1}$; and −44/−42 followed by −17 (w), 12 (s), 35/38 (s), 59/62 (w), 88 (s), and 116 (s) cm$^{-1}$]. The very rich intermolecular Franck−Condon activity of the $BA_2$ cluster indicates a large change in the geometry of the cluster following the electronic excitation of the cluster.

In the $BA_3^+$ channel, an origin (doublet) with a much larger red shift (−101/−99 cm$^{-1}$) appears with two well-defined vdw progressions with small band spacings of 7 cm$^{-1}$ [−101/−99, −94/−93, −87/−85, −80/−79, −76/−75, −68/−67, and −62/−61 cm$^{-1}$], and 10 cm$^{-1}$ [−101/−99 followed by −91/−89, −80/−79, and −72/−71 cm$^{-1}$]. Fragmentation by a loss of single acetic acid from the photoionized $BA_4^+$ cluster results in the appearance of frequencies corresponding to the $BA_4$ cluster in the $BA_3^+$ mass channel.

A strong doublet origin for the $BA_4$ cluster appears in the $BA_4^+$ channel, blue shifted from the benzene $6_0^1$ origin by 14/16 cm$^{-1}$, and accompanied by two well-resolved vdw progressions [a strong progression at 24/26, 33/35, 42/43, and 53/55 cm$^{-1}$, intermingled with a weaker progression at 17/19, 27/29, and 36/38 cm$^{-1}$]. Other small vdw bands also appear at 40, 45, 51, and 56 cm$^{-1}$.

In the $BA_5^+$ channel, no characteristic features can be unambiguously assigned to the $BA_5$ cluster due to the weak signal levels, which result from the very low concentration of the $BA_5$ cluster in the beam. The major features observed in this channel are due to fragmentation products from the $BA_6$ cluster, which appear at −15/−13 and −7 cm$^{-1}$. However, a weak doublet at −87/−85 cm$^{-1}$ can be tentatively assigned to the $BA_5$ origin, followed by two vdw bands at −73/−72 cm$^{-1}$ and −61/−62 cm$^{-1}$. In the $BA_6^+$ channel, we assign two strong origins at −15/−13 cm$^{-1}$ (origin I, with vdw bands at 5/7 and 23/25 cm$^{-1}$) and −7/−4 cm$^{-1}$ (origin II, with a vdw doublet at 14/17 cm$^{-1}$).

Figure 2 displays the integrated ion intensities of the $BA_n^+$ mass channels as a function of $n$ within the region of −110 to +150 cm$^{-1}$ from the $6_0^1$ transition of benzene. The integrated ion intensities are corrected for fragmentation of the photoionized clusters by summing the ion intensities appearing at the

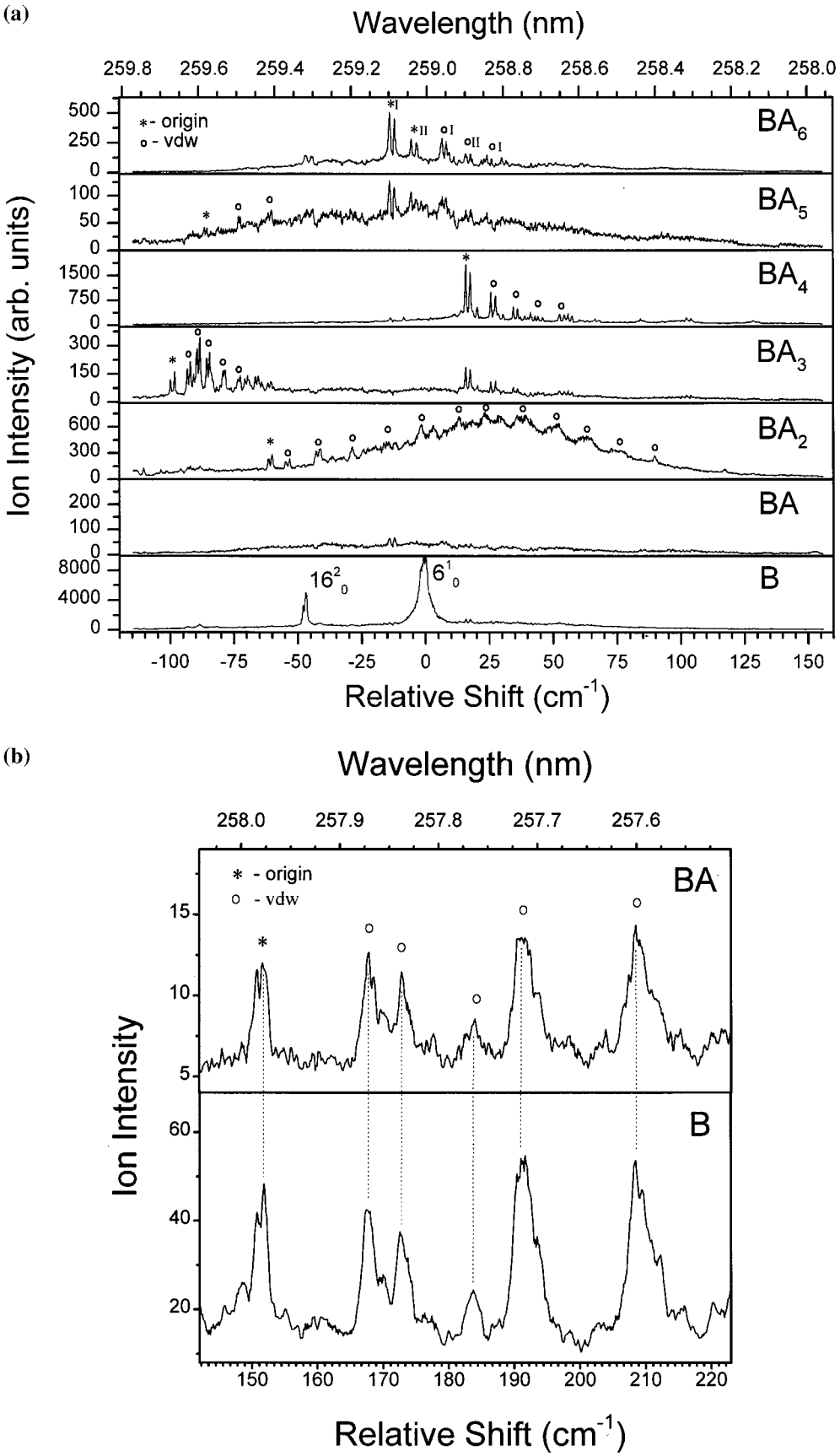


**Figure 1.** (a) One-color resonant two-photon ionization spectra of $C_6H_6(CH_3COOH)_n$, $BA_n$, with $n = 1$ through 6. (b) One-color resonant two-photon ionization spectrum of the $C_6H_6(CH_3COOH)$ complex, BA, monitoring the $B^+$ and $BA^+$ mass channels.

same frequency in channels ($n$) and ($n + 1$), and assigning them to the higher mass channel ($n + 1$). The resulting data reveals strong even/odd alternation in the ion intensities within the resonance absorption region of the clusters, with the even clusters 2, 4, and 6 being more abundant than the odd clusters 1, 3, and 5.

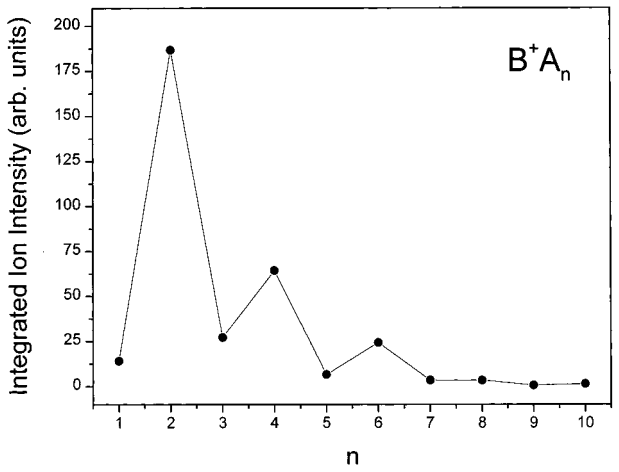


**Figure 2.** Integrated ion intensities of the $C_6H_6(CH_3COOH)_n$ mass channels, $BA_n^+$, as a function of $n$ within the region $-110$ to $+250$ $cm^{-1}$ with respect to the $6_0^1$ transition of $C_6H_6$.

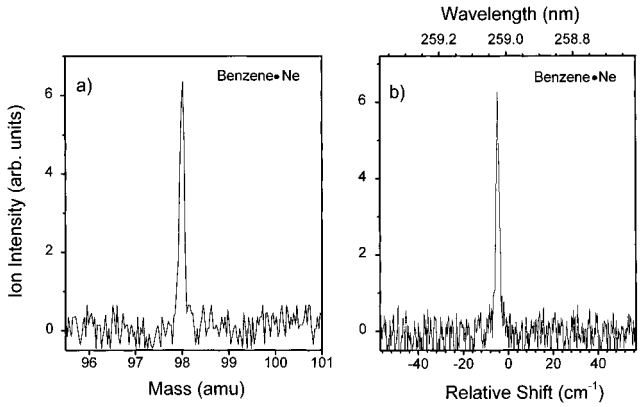


**Figure 3.** Mass spectrum of the $C_6H_6$•(Ne) complex. One-color resonant two-photon ionization spectrum of the $C_6H_6$•(Ne) complex.

Some new features are observed only when using Ne as the carrier gas in the supersonic expansion instead of He. The first feature is the appearance of a new mass peak at *m/z* 98, as shown in Figure 3a, corresponding to the $C_6H_6$•(Ne) complex. This complex shows a single origin red shifted from the $6_0^1$ transition of benzene by 4.9 $cm^{-1}$ as shown in Figure 3b. This assignment is in agreement with previous work using laser-induced fluorescence where the $C_6H_6$•(Ne) red shift has been estimated as 3−5 $cm^{-1}$.[36,37] The second feature observed only when using Ne as a carrier gas is the appearance of new peaks in the $BA_4^+$ and $BA_6^+$ mass channels corresponding to red shifts of ≈4 $cm^{-1}$ from the $BA_4$ and $BA_6$ origins (only origin II of the $BA_6$ cluster). The red shifted peaks also appear in the accompanied vdw modes of the assigned origins, as shown in Figure 4 for the $BA_4$ cluster. The appearance of these new red-shifted bands depends on the Ne pressure in the expansion vapor mixture. At the lowest neon pressure used in the supersonic expansion (10 psi), no additional peaks are observed. We assign the new red-shifted doublets observed in the $BA_4^+$ and the $BA_6^+$ mass channels to $C_6H_6$•(Ne)•$(CH_3COOH)_4$, and $C_6H_6$•(Ne)•$(CH_3COOH)_6$ clusters, respectively. Upon photoionization, these clusters fragment efficiently (100%) by loss of a Ne atom and appear in the $BA_4^+$ and $BA_6^+$ mass channels. It is interesting to note that the attachment of a Ne atom appears to be more pronounced for the $BA_4$ and $BA_6$ clusters. For the $BA_2$ cluster, the absence of sharp peaks in the R2PI spectrum makes it difficult to conclusively rule out the formation of the $C_6H_6$•(Ne)•$(CH_3COOH)_2$ cluster. However, for the BA, $BA_3$, and $BA_5$ clusters, no changes are detected in the R2PI spectra when using Ne as a carrier gas instead of He.

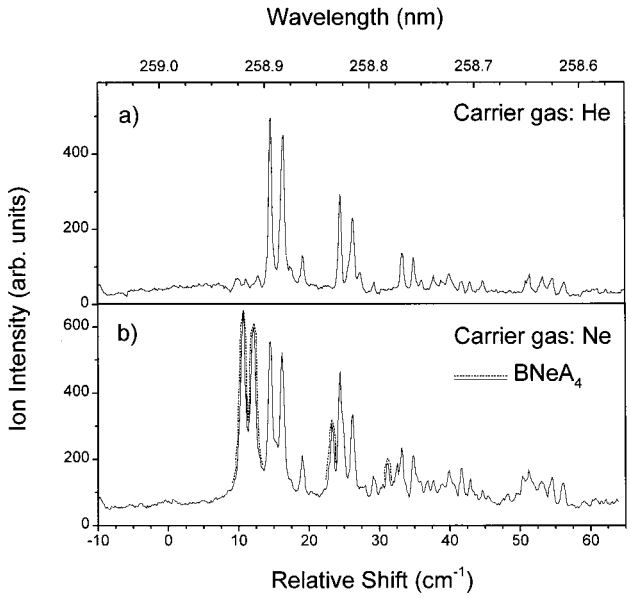


**Figure 4.** One-color resonant two-photon ionization spectrum of the $C_6H_6(CH_3COOH)_4$ cluster, $BA_4$, generated using (a) He, or (b) Ne, as a carrier gas in the supersonic expansion.

## 4. Discussion

The observation of a strong even/odd alternation in the integrated ion intensity within the absorption region of the $BA_n$ clusters indicates that clustering of preformed dimers is the major association channel in the nucleation kinetics of supersaturated acetic acid vapor. The formation of $BA_n$ clusters containing an even number of acetic acid molecules is therefore a result of multiple association of the hydrogen-bonded dimers. We assume that the presence of benzene does not change the clustering mechanism of acetic acid vapor (typically the B/A ratio in preexpansion mixture is ≈$10^{-4}$). The high concentration of acetic acid dimer in the preexpansion vapor mixture is expected to enhance the formation of the even clusters by the sequential addition of dimers. It should be clear that the clustering of dimers could lead to the formation of intact tetramers and higher clusters by hydrogen bonding either as cyclic or open chain structures. The small intensity of the BA cluster can be explained by a fast depletion of the BA clusters through the generation of $BA_2$ and $BA_3$ by the addition of acetic acid monomer and dimer, respectively. This does not normally happen in clustering of unassociated vapors since the monomer concentration is typically too high to result in any significant depletion effect.

The spectral shifts from the $6_0^1$ origin of the isolated benzene molecule imposed by acetic acid clusters provide information on the nature of the intermolecular interactions within the binary clusters. The strong blue shift observed for the BA cluster (+152 $cm^{-1}$) is consistent with hydrogen bonding interaction between the OH group of acetic acid and the $\pi$-electron system of the benzene ring. For example, benzene complexes with $H_2O$, $CH_3OH$, HCl, and $CHCl_3$ exhibit blue shifts of 52, 44, 125, and 179 $cm^{-1}$, respectively.[7,11,38,39] The efficient fragmentation observed for the BA complex following photoionization is a direct consequence to the $\pi$-hydrogen bonded geometry in the neutral complex. The structural change from the $\pi$-hydrogen bonding in the neutral species to the predominantly ion−dipole interaction in the ionized species involves a great strain, which leads to efficient fragmentation.

We also note that the $BA_2$ and $BA_3$ clusters exhibit strong red shifts of $-60$ and $-100$ $cm^{-1}$, respectively, while the $BA_4$ and $BA_6$ clusters show small blue and red shifts of $+14$ and $-14$ $cm^{-1}$, respectively. The strong red shifts are suggestive of predominantly dispersion interactions, consistent with stacked structures where the benzene is surface-attracted to the acetic acid clusters.

The small red shift of the $C_6H_6$·(Ne) complex indicates that excited state binding energy is slightly larger by $\approx 5$ $cm^{-1}$ than the ground-state binding energy. The similarity in the red shifts found for the benzene·(Ne) [with respect to the $6_0^1$ transition of benzene] and for the benzene·(Ne)·(acetic acid)$_4$ [with respect to the origin of the benzene−(acetic acid)$_4$], strongly suggests that the benzene···(acetic acid)$_4$ interaction is not affected by the weak benzene···Ne interaction. A similar situation has been found for the (Ne)·$C_6H_6$·($H_2O$) cluster, where a rotational spectrum has revealed that benzene is sandwiched between the Ne atom and the $H_2O$ molecule in a symmetric top structure.[40,41] A similar structure could be proposed for the (Ne)·$C_6H_6$·(acetic acid)$_4$ or the (Ne)·$C_6H_6$·(acetic acid)$_6$ clusters, where benzene experiences a weak Ne···benzene interaction on one side and a stronger benzene···(acetic acid)$_4$ or benzene···(acetic acid)$_6$ interaction on the other side. A *multilayer* cluster consisting of a benzene molecule stacked with a Ne atom on the top and two or three acetic acid dimers on the bottom may be considered. Such stacked assemblies allow the interaction between Ne and $C_6H_6$ to remain essentially the same as that of the $C_6H_6$·(Ne) complex. Ab initio and density functional theory calculations are currently in progress in order to gain further insight into the structures of the $BA_n$ species including the Ne-containing clusters.[42]

## 5. Conclusions

The R2PI spectra of benzene−acetic acid binary clusters $BA_n$, with $n = 1-6$ have been reported. The results indicate that cluster formation from acetic acid vapor proceeds mainly via the association of preformed hydrogen-bonded dimers. The spectral shift of the BA complex is consistent with $\pi$-hydrogen bonding interaction with the benzene ring. The spectral shifts of the $BA_2$ and $BA_3$ clusters are consistent with a predominantly dispersion interaction which is enhanced upon electronic excitation of the benzene molecule. The R2PI spectrum of the $C_6H_6$·(Ne) complex reveals a small red shift of $\approx 5$ $cm^{-1}$, in good agreement with previous work. Spectroscopic evidence for the formation of (Ne)·($C_6H_6$)·($CH_3COOH$)$_4$ and (Ne)·($C_6H_6$)·($CH_3COOH$)$_6$ clusters has been presented. The direction and magnitude of the spectral shifts indicate that the $C_6H_6$···Ne and the $C_6H_6$···($CH_3COOH$)$_4$ or the $C_6H_6$···($CH_3COOH$)$_6$ structures are retained in the multicomponent clusters, suggesting little perturbation due to the weak $C_6H_6$···Ne interaction. Theoretical calculations are currently in progress in order to gain further insight into the structures of these clusters.

**Acknowledgment.** The authors gratefully acknowledge financial support from NSF Grant No. CHE 9816536. Acknowledgment is also made to the donors of the Petroleum Research Fund, administered by the American Chemical Society, and to the Jeffress Memorial Trust for the partial support of this research.

## References and Notes

(1) Castleman, A. W., Jr.; Bowen, K., Jr. *J. Phys. Chem.* **1996**, *100*, 12911.
(2) Castleman, A. W., Jr.; Wei, S. *Annu. Rev. Phys. Chem*. **1994**, *45*, 685.
(3) Kim, S. K.; Li, S.; Bernstein, E. R. *J. Chem. Phys*. **1991**, *95*, 3119.
(4) Schutz, M.; Burgi, T.; Leutwyler, S.; Fischer, T. *J. Chem. Phys*. **1993**, *98*, 3763.
(5) Stanley, R. J.; Castleman, A. W., Jr. *J. Chem. Phys*. **1993**, *98*, 796.
(6) Burgi, T.; Droz, T.; Leutwyler, S. *Chem. Phys. Lett*. **1995**, *246*, 291.
(7) Garrett, A. W.; Severance, D. L.; Zwier, T. S. *J. Chem. Phys.* **1992**, *96*, 7245.
(8) Pribble, R. N.; Zwier, T. S. *Science* **1994**, *265*, 75.
(9) Liu, K.; Brown, M. G.; Saykally, R. J.; Clary, D. *Nature* **1996**, *391*, 591.
(10) Gruenloh, C. J.; Carney, J. R.; Arrington, C. A.; Zwier, T. S.; Fredericks, S. Y.; Jordan, K. D. *Science* **1997**, *276*, 1678.
(11) Garrett, A. W.; Severance, D. L.; Zwier, T. S. *J. Chem. Phys*. **1992**, *96*, 7245.
(12) Daly, G. M.; Schultz, C.; Castevens, C.; Shillady, D. D.; El-Shall, M. S. In *Science and Technology of Atomically Engineered Materials*; Jena, P., Khanna, A. N., Rao, B. K., Eds.; World Scientific: New Jersey, 1996; p 251.
(13) Karle, J.; Brockway, L. O. *J. Am. Chem. Soc*. **1944,** *66*, 574.
(14) Ritter, H. L.; Simons, J. H. *J. Am. Chem. Soc.* **1945**, *67*, 757.
(15) Johnson, E. W.; Nash, L. K. *J. Am. Chem. Soc.* **1950**, *72*, 548.
(16) Taylor, M. D. *J. Am. Chem. Soc*. **1951**, *73*, 315.
(17) Taylor, M. D.; Bruton, J. *J. Am. Chem. Soc.* **1952**, *74*, 4151.
(18) Weltner, W., Jr. *J. Am. Chem. Soc.* **1955**, *77*, 3941.
(19) Potter, A. E., Jr.; Bender, P.; Ritter, H. L. *J. Phys. Chem.* **1955**, *59*, 250.
(20) Christian, S. D.; Affsprung, H. E.; Lin, G. *J. Chem. Soc*. **1964**, 1848.
(21) Mathews, D. M.; Sheets, R. W. *J. Chem. Soc. A* **1969**, 2203.
(22) Kolysko, L. E.; Gorodinskaya, E. Ya. *Russ. J. Phys. Chem*. **1973**, *47*, 737.
(23) Hagler, T.; Dauber, P.; Lifson, S. *J. Am. Chem. Soc.* **1979**, *101*, 5131.
(24) Cook, K. D.; Taylor, J. W. *Int. J. Mass Spectrom. Ion Phys*. **1980**, *35*, 259.
(25) Frurip, D. J.; Curtiss, L. A.; Blander, M. *J. Am. Chem. Soc.* **1980**, *102*, 2610.
(26) Chao, J.; Zwolinski, B. J. *J. Phys. Chem. Ref. Data* **1978**, *7*, 363.
(27) Bertagnolli, H. *Chem. Phys. Lett.* **1982**, *93*, 287.
(28) Sievert, R.; Cadez, I.; Van Doren, J.; Castleman, A. W., Jr. *J. Phys. Chem*. **1984**, *88*, 4502.
(29) Keesee, R. G.; Sievert, R.; Castleman, A. W., Jr. *Ber. Bunsen-Ges. Phys. Chem.* **1984**, *88*, 273.
(30) Mori, Y.; Kitagawa, T. *Inter. J. Mass Spectrom. Ion Proc*. **1988**, *84*, 319.
(31) Faubel, M.; Kisters, Th. *Nature* **1989**, *339*, 527.
(32) Wilcox, C. F.; Bauer, S. H. *J. Chem. Phys.* **1997**, *107*, 5794.
(33) El-Shall, M. S.; Yu, Z. *J. Am. Chem. Soc.* **1996**, *118*, 13058.
(34) El-Shall, M. S.; Daly, G. M.; Yu, Z.; Meot-Ner, M. *J. Am. Chem. Soc*. **1995**, *117*, 7744.
(35) Atkinson, G. H.; Parmenter, C. S. *J. Mol. Spectrosc*. **1978**, *73*, 20; 31; 52.
(36) Hobza, P.; Selzle, H. L.; Schlag, E. W. *Chem. Rev*. **1994**, *94*, 1767.
(37) Stephenson, T. A.; Rice, S. A. *J. Chem. Phys*. **1984**, *81*, 1083.
(38) Gotch, A. J.; Zwier, T. S. *J. Chem. Phys.* **1990**, *93*, 6977.
(39) Gord, J. R.; Garrett, A. W.; Bandy, R. E.; Zwier, T. S. *Chem. Phys. Lett*. **1990**, *171*, 443.
(40) Arunan, E.; Emilsson, T.; Gutowsky, H. S. *J. Chem. Phys.* **1993**, *99*, 6208.
(41) Arunan, E.; Emilsson, T.; Gutowsky, H. S. *J. Chem. Phys.* **1994**, *101*, 861.
(42) Germanenko, I. N.; El-Shall, M. S. *J. Phys. Chem*., to be submitted.